Scalable approach for lensless imaging at x-ray wavelengths

S. Eisebitt,[a] M. Lörgen, and W. Eberhardt
BESSY m.b.H., Albert-Einstein-Strasse 15, 12489 Berlin, Germany

J. Lüning, S. Andrews, and J. Stöhr
SSRL, Stanford Linear Accelerator Center, 2575 Sand Hill Road, Menlo Park, California 94025

(Received 1 December 2003; accepted 3 March 2004)

We demonstrate a versatile approach to perform lensless imaging at x-ray wavelength. A special design of a sample holder allows recovery of the low spatial frequency information of the sample from the Patterson map of the measured diffraction. As a result, the phase can be reconstructed from an oversampled x-ray diffraction pattern alone, eliminating the need to resort to a low-resolution image of the sample. As the sample holder provides this functionality due to a suitable reference hole, the technique is applicable to a wide variety of samples and can be easily scaled to investigate large arrays of samples. The method is especially well suited for single-shot experiments as envisioned with x-ray free-electron lasers. © *2004 American Institute of Physics.*
[DOI: 10.1063/1.1728320]

In a *coherent* scattering experiment with spatially oversampled detection, it is possible to solve the phase problem, i.e., the phase of the scattered radiation at the detector can be retrieved.[1–3] As a result, it is possible to *image* a specimen, while only statistical information about a sample can be obtained in incoherent scattering. This technique is often called ''lensless imaging'' or ''oversampling phasing.'' As in conventional imaging microscopy, the spatial resolution is ultimately limited by the wavelength of the radiation (or particle) used. Consequently, there is a strong incentive to carry out such experiments at short wavelengths beyond the visible spectral range. Over the last 5 years there has been significant experimental progress in performing lensless imaging at x-ray wavelengths, exploiting the high brilliance of synchrotron radiation sources. A spatial resolution below 10 nm as well as tomographic imaging have been reported.[4–9] The next generation of synchrotron radiation facilities—free-electron x-ray lasers—will deliver a coherent photon flux many orders of magnitude higher than available today.[10] This will facilitate stroboscopic lensless imaging with increased spatial resolution using single x-ray pulses on a femtosecond time scale.

A general experimental problem, however, is the fact that it is practically impossible to collect reliable scattering data at or close to zero momentum transfer ($\mathbf{q}=0$). This is due to the facts that (a) transmission is superimposed on forward scattering and (b) most existing two-dimensional (2D) spatially resolving detectors are not capable of imaging the very high dynamic range encountered close to $\mathbf{q}=0$. As a result, experiments are typically performed with a central beam stop. As a consequence, low spatial frequency information is not available from the scattering experiment and has to be obtained by complementary techniques such as optical microscopy.[4] A special solution to this problem has been proposed by Fienup,[3] based on the convolution theorem as applied to a diffraction experiment: the Fourier transform of the diffraction pattern (also known as the Patterson map) is identical to the spatial autocorrelation of the diffracting object. If the object is prepared in a suitable way, the missing low spatial frequency information can be extracted from the Patterson map. This approach has recently been applied using x rays by He *et al.*[11] In Ref. 11, the object consisted of gold balls 50 nm in diameter. Employing a scanning tunneling microscope (STM), the balls are arranged such that one ball is separated from the others. As a result, there is a region in the Patterson map where this isolated ball ''images'' the remainder of the object, allowing one to extract the shape of this remaining part and thus providing the low spatial frequency information needed for a successful phase retrieval. Obviously, this approach of preparing the object with an STM has a limited applicability with regard to the type of specimen which can be investigated.

In this letter we propose and demonstrate a technique which overcomes these limitations and thus allows lensless imaging for a wide variety of samples based on x-ray diffraction data alone. We also take advantage of the convolution theorem, but in our case it is not the sample itself but a suitable microstructured sample holder that allows us to couple the diffraction from the object of interest to the diffraction from a spatially separated, small reference object. Such a sample holder could be based on a lithographically patterned Au film deposited on a silicon nitride membrane, such that the Au blocks the x-ray beam while the uncovered membrane has a high x-ray transmission. The structure could consist of a sample area $5\ \mu\mathrm{m}\times 5\ \mu\mathrm{m}$ in size and a reference hole of $0.1\ \mu\mathrm{m}$ diameter, offset by $8\ \mu\mathrm{m}$ to the side. If a specimen is placed in the sample area and the entire structure is illuminated coherently, the low spatial frequency of the sample can be directly obtained from the Patterson map, as the sample is imaged with the resolution equal to the size of the reference structure. With this low-resolution input information, an iterative phase retrieval algorithm can be used to obtain an image of the sample with higher resolution.

As a proof of principle experiment for this approach, we have generated the test structure shown in the scanning electron micrograph in Fig. 1(a). The structures were written

[a]Electronic mail: eisebitt@bessy.de

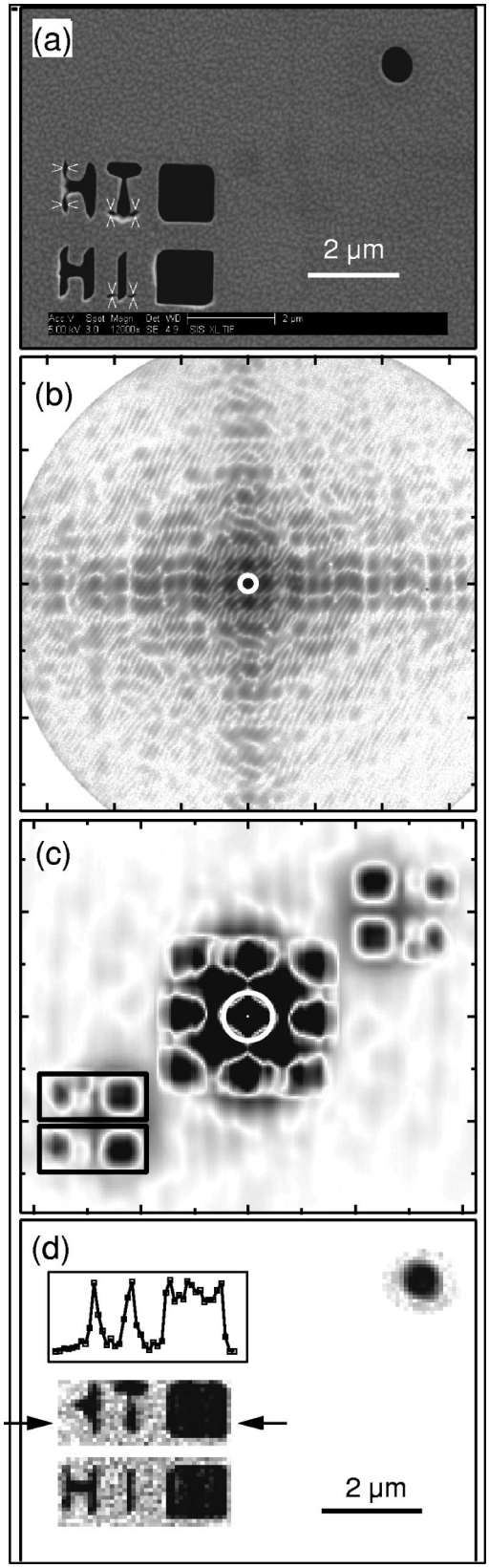

FIG. 1. (a) Scanning electron micrograph of the test sample, containing the sample region (letters and squares) and the reference hole. (b) Coherent diffraction pattern on a logarithmic intensity gray scale over a range $-35\ \mu\mathrm{m}^{-1} \leq q \leq 35\ \mu\mathrm{m}^{-1}$. The central maximum indicated by the white circle was recorded but not used in the data analysis. (c) Patterson map obtained by Fourier transformation of (b) shown over a $\pm 8.5\ \mu$m horizontal and $\pm 7.5\ \mu$m vertical range. The regions indicated by two black rectangles and a white circle were chosen for image reconstruction in (d) (''support regions''). (d) Image reconstruction based solely on the x-ray diffraction pattern in (b), using the support regions shown in (c). Inset: scan line between the arrows.

with a focused ion beam (FIB) into a free-standing gold film of 2 μm thickness. The sample consists of a ''H,'' an ''I,'' and an open square, cut through the gold film and repeated in two lines. This test structure is contained within an area of 3.3 μm$\times$3.7 μm. A reference hole 0.8 μm in diameter was placed at a distance of 5 μm to the sample pattern.

Coherent x-ray scattering from this test sample was recorded in transmission geometry at beamline UE56-1/SGM at the BESSY synchrotron facility. Soft x rays with a wavelength of $\lambda = 3.1$ nm were used. To satisfy both longitudinal and transverse coherence requirements the undulator radiation is monochromatized and then spatially filtered. With an energy bandwidth of $\lambda/\Delta\lambda \approx 5000$, the longitudinal coherence length is given by $\xi_l = \lambda^2/2\Delta\lambda \approx 8\ \mu$m, which is much larger than any possible optical path length differences in our setup. The spatial filter consists of a pinhole of $d = 50\ \mu$m diameter, positioned at a distance $L = 0.723$ m upstream of the sample. The transverse coherence length at the sample position defined by this geometry is $\xi_t = \lambda L/\pi d \approx 13\ \mu$m, so that the sample and the reference hole, which lie within an area of 7 μm$\times$9 μm, are illuminated coherently. A 2D position-sensitive detector is placed 0.990 m downstream of the sample. The detector is based on a stack of five microchannel plates coated with a CsI layer for photon-to-electron conversion and a 2D resistive anode readout, resulting in a 100 μm$\times$100 μm pixel size.

The coherent scattering pattern from this sample is shown in Fig. 1(b). As the sample is a real object, the scattered intensity is centro-symmetric. The vertical and horizontal cross-like intensity pattern originates from the perpendicular structures in the letters and the squares. A high-frequency line pattern can be observed along the diagonal lines of the central cross. This component is due to interference of x rays passing through the reference pinhole with x rays passing through the letter pattern. Due to the general limitations mentioned above, in the data analysis we do not use the center part of the diffraction pattern marked by a circle in Fig. 1(b). At 3.1 nm x-ray wavelength the detector covers a momentum transfer $q_{\max}$ of approximately 35 $\mu\mathrm{m}^{-1}$ in our experimental geometry, corresponding to a maximum spatial resolution of 180 nm.

In order to reconstruct the real-space structure of the sample from the coherent diffraction pattern the phase problem has to be solved. We use the measured intensity pattern as input to an iterative reconstruction algorithm of Gerchberg–Saxton type,[1,5] starting with random phases. The oversampling rate in the scattering image can be determined experimentally from the high-frequency oscillations generated by the beating of the reference hole with the letter pattern. We measure four resolvable elements per oscillation period and thus an oversampling of four per linear axis compared to sampling with one data point per period. The total oversampling in our 2D scattering experiment is thus 16. From a mathematical standpoint, an oversampling larger than two is sufficient for a reconstruction of the phase in the scattered wave field.[1,2,12] In practice, larger oversampling is needed in order to produce some redundancy which allows one to compensate for possible experimental limitations. Note that the sample region has been illuminated coherently with a transverse coherence that approximately matches the

oversampling, i.e., in any linear direction the transverse coherence length is about as large as the sample size times the 1D oversampling factor.

The constraints applied in the phase reconstruction algorithm are (a) in real space: no scattering intensity originates from outside the support, i.e., from the opaque gold film; (b) in Fourier space: the intensities correspond to the experimental data.

The support contains the lowest spatial frequency information about the object, i.e., where the object is placed and its rough outline. We use the autocorrelation of the real-space object, Fig. 1(c), to determine the support shape from the coherent diffraction data alone.[11] According to the convolution theorem the square of the Fourier modulus of an object is equal to the Fourier transform of the autocorrelation of the same object. The inverse Fourier transform of the measured diffraction pattern, also known as Patterson map, therefore shows the autocorrelation of the real-space object. This is shown in Fig. 1(c). The region where the reference hole convolves the two rows of letters is clearly visible: the two rows and within those the positions of the letters and the square can be identified. The spatial resolution of this image is given by the diameter of the reference hole. Solely on the basis of this autocorrelation we choose the support region for the iterative phase retrieval as the areas within the two black rectangles and the white circle marked in Fig. 1(c). While the rectangles contain the sample structures, the circle contains the region where the reference pinhole convolves itself, which is by definition at the origin of the 2D autocorrelation. Note that the selection of these support regions does not use any *a priori* knowledge of the real-space structures, e.g., the presence of letters aligned in rows.

Using this support, the phase is retrieved by a modified Gerchberg–Saxton algorithm, known as the Fienup error reduction algorithm.[13] No information from the real-space image in Fig. 1(a) is used in the reconstruction procedure. After 300 iterations we obtain the intensity map shown in Fig. 1(d), which clearly is an image of our test sample. The overall structure and most of the fine structure in the letter pattern is well reproduced. Several sample features marked by fine-line arrows in the SEM picture are not reproduced in the image reconstruction. These features have a characteristic width of 100 nm and are thus below the smallest structure size resolvable due to the maximum momentum transfer in the setup used here. We obtain the same reconstructed image for different random start phases or when alternatively employing a phase retrieval algorithm on the basis of a hybrid input–output scheme.[13] By comparison with the SEM image and from the scan line through the reconstructed image, we determine the spatial resolution obtained in the lensless imaging to be 180 nm, i.e., momentum transfer limited.

We have thus achieved a phase retrieval and image reconstruction based on coherent x-ray scattering data alone, without having to resort to other information about the sample such as a light microscopy image. The only input used in addition to the measured scattering pattern is the knowledge that the sample is opaque outside the structured area and that a reference hole exists in this otherwise opaque region. The location and shape of this support region can be determined from the experimental data due to the presence of the reference hole, using the convolution theorem. A high-resolution image of the structures within the support region is obtained by subsequent iterative phase retrieval. This reference hole approach is versatile and scalable and can thus be applied to a wide variety of specimen.

If the region containing the letters in our test experiment is replaced by a membrane with high x-ray transmission for the wavelength used in a scattering experiment, one obtains a sample holder into which a variety of specimen can be introduced and imaged. Such a structure can be fabricated using standard lithography and Si_3N_4 membrane technology. If necessary, smaller reference holes can be produced by FIB sputtering after the lithographic definition of the sample windows. Nanoparticles, colloids, or biological samples can be introduced in this structure by employing integrated light microscopy/manipulator stages as used for microinjection in biotechnology, which achieve sub-μm manipulation resolution. With suitable μm precision shutters, thin film samples could be grown on the silicon nitride membrane while keeping the reference hole open. Wafers containing a multitude of these sample/reference structures could be preloaded with samples *ex situ*, and introduced in an experimental chamber for measurement, enabling high throughput investigations. We believe that this approach will be especially valuable if lensless imaging matures to a standard technique. The availability of a sample array for lensless imaging will be particularly important for investigations as envisioned with free electron x-ray lasers. Due to the high coherent photon flux in these devices, the sample can be imaged stroboscopically on a femtosecond time scale using a single x-ray pulse. Many types of samples will be damaged (after they have been imaged) by the x-ray pulse. A large array of samples with integrated reference holes is thus important for quasicontinuous operation of a lensless imaging facility at a free-electron laser.

S.A. would like to thank the Fannie and John Hertz Foundation for financial support. The research of J.L. and J.S. is supported by the Office of Basic Energy Sciences of the U.S. Department of Energy.

[1] R. W. Gerchberg and W. O. Saxton, Optik (Stuttgart) **35**, 237 (1972).
[2] J. R. Fienup, Appl. Opt. **21**, 2758 (1982).
[3] J. R. Fienup, J. Opt. Soc. Am. A **4**, 118 (1987).
[4] J. W. Miao, P. Charalambous, J. Kirz, and D. Sayre, Nature (London) **400**, 342 (1999).
[5] J. A. Pitney, I. A. Vartanyants, and I. K. Robinson, Digital image recovery and synthesis IV **3815**, 1999 (1999).
[6] I. K. Robinson, I. A. Vartanyants, G. J. Williams, M. A. Pfeifer, and J. A. Pitney, Phys. Rev. Lett. **87**, 195505 (2001).
[7] I. A. Vartanyants and I. K. Robinson, J. Phys.: Condens. Matter **13**, 10593 (2001).
[8] J. Miao, T. Ishikawa, B. Johnson, E. H. Anderson, B. Lai, and K. O. Hodgson, Phys. Rev. Lett. **89**, 088303 (2002).
[9] J. Miao, T. Ishikawa, E. H. Anderson, and K. O. Hodgson, Phys. Rev. B **67**, 174104 (2003).
[10] A. Cho, Science **296**, 1008 (2002).
[11] H. He, S. Marchesini, M. Howells, U. Weierstall, H. Chapman, S. Hau-Riege, A. Noy, and J. C. H. Spence, Phys. Rev. B **67**, 174114 (2003).
[12] H. Stark, *Image Recovery: Theory and Applications* (Academic, New York, 1987).
[13] J. R. Fienup, Opt. Lett. **3**, 27 (1978).